Materials Chemistry and Physics 314 (2024) 128837

Contents lists available at ScienceDirect

Materials Chemistry and Physics

journal homepage: www.elsevier.com/locate/matchemphys

Development and implementation of holmium sources produced by molecular plating for the HOLMES experiment

N. Cerboni [a], G. de Bodin-de Galembert [a], M. De Gerone [b], G. Gallucci [b], E. Müller [a], A. Nucciotti [c,d], P. Steinegger [a], E.A. Maugeri [a,*]

[a] Paul Scherrer Institute (PSI), Villigen, Switzerland
[b] Istituto Nazionale di Fisica Nucleare (INFN), Sezione di Genova, Genova, Italy
[c] Dipartimento di Fisica, Università degli studi di Milano-Bicocca, Milano, Italy
[d] Istituto Nazionale di Fisica Nucleare, Sezione di Milano-Bicocca, Milano, Italy

HIGHLIGHTS

- The neutrino mass direct measurement is a paramount objective in contemporary science.
- The utilization of a Ho-163 source plays a pivotal role in neutrino mass measurement.
- Successful fabrication of a Ho source was achieved through molecular plating method.

ARTICLE INFO

Keywords:
Thin layers
Molecular plating
Holmium
Ion source

ABSTRACT

This manuscript reports on the optimization of a molecular plating procedure for the production of uniform and homogeneous films of holmium deposited onto gold-plated copper substrate. In particular, the effects caused by molecular plating solvents with different vapour pressure on the morphology and stability of the resulting films were investigated, allowing the selection of the optimum solvent. The developed procedure will allow allow the production of sources of holmium ions for the envisaged HOLMES experiment aiming at the direct measurement of the neutrino mass.

1. Introduction

HOLMES is an experiment for the direct measurement of the neutrino mass by the calorimetric measurement of the energy released during the electron capture decay of ^{163}Ho [1], based on the idea originally suggested by De Rujula and Lusignoli in 1982 [2].

In particular, about 6.24×10^{16} atoms of ^{163}Ho will be implanted into the detector system, an array of about 1000 transition edge sensor based microcalorimeters, allowing for the direct measurement of the total energy released from the decay, excluding the fraction carried by the neutrino. The difference between the experimentally measured energy at the end-point and the theoretical Q-value of the electron capture decay will give an accurate estimation of the electron neutrino rest mass.

^{163}Ho will be produced via thermal neutron irradiation of 30% isotopically enriched $^{162}Er_2O_3$ at the Institut Laue-Langevin (ILL, Grenoble, France), chemically purified at the Paul Scherrer Institut (PSI, Villigen, Switzerland) [3], mass separated from ^{166m}Ho, which is co-produced during the neutron irradiation, and implanted into the detectors using an ion implanter developed at the Genova INFN laboratory (Genova, Italy) [4]. More precisely, holmium, integrated in a solid source, will be atomized and ionized via penning sputtering, before being mass separated and then implanted as Ho^+ into the detector array [5].

The solid source, hereafter referred to as holmium source, should preferably contain holmium either in its metallic state or as a chemical holmium compound that decomposes into its constituents when exposed to the plasma. Additionally, the holmium species must be homogenously and uniformly distributed along the surface of the source to ensure a constant and controlled release of atoms during the sputtering.

According to the original project, the holmium source should have been produced following a three-steps process [1]. The first step consisted of the reduction of Ho_2O_3, which is the chemical form of holmium

* Corresponding author.
E-mail address: emilio-andrea.maugeri@psi.ch (E.A. Maugeri).

https://doi.org/10.1016/j.matchemphys.2023.128837
Received 16 August 2023; Received in revised form 22 November 2023; Accepted 17 December 2023
Available online 18 December 2023

after its chemical purification, to its metal form, Ho^0, at 1600 °C in the presence of metallic yttrium. During the second phase, the vapour of metallic holmium produced at this temperature, should be condensed onto a gold-coated quartz substrate. Finally, the holmium-gold mixture should be scratched from the quartz substrate and used as holmium source in form of powder. In a test experiment, performed in 2019 using natural holmium [5,6], an estimated yield of about 80%, obtained measuring the mass of material condensed onto the quartz substrate, was estimated. This evaluation was not supported by a chemical characterization of the deposited species. Thus, the condensation of other elements, present as contaminants in the source, or the presence of holmium in other chemical forms, rather than the elemental one, cannot be excluded. Furthermore, the authors proposed an additional step, consisting in the sintering of holmium with titanium, nickel and tin to obtain a metallic cathode to be used as holmium source. No yield was reported for this step. In conclusion, the proposed process was characterized by several steps, with not well-defined yields, performed at high temperatures, which is a critical issue when working with the radioactive ^{163}Ho isotope for radioprotection reasons. Therefore, we propose an alternative, one-step method working at room temperature, with almost quantitative yields, requiring very simple and easy-to-handle equipment, i.e. molecular plating.

Molecular plating (MP) is a well know method [7] for producing thin, homogeneous films with uniform thickness, composed of elements with a reduction potential more negative than water, such as actinides [7–13], rare-earth elements [14–16] and alkaline earth metals [17]. Those elements cannot be electroplated as metal coatings on an electrode/backing when dissolved in aqueous solutions, since water would be rapidly reduced at the required potentials. The consequent development of large amount of gaseous hydrogen would prevent a homogeneous deposition of the element, even if reduced to its zero oxidation state. MP is usually performed in a two electrodes setup, using an organic electrolyte, and it can be performed both in galvanostatic or potentiostatic mode. This method has been mainly used for producing standard sources for α-spectroscopy [18–21], targets for nuclear physics experiments [17,22,23] and studies on superheavy elements chemistry [24–26].

Homogeneity and adhesion of the deposited film produced by MP depend on several parameters, such as applied voltage, current density, plating time, surface density of the deposited species, temperature of the electrolyte, and morphology of the cathode. The choice of the plating solvent, which is strongly related to the chemistry of the element to be deposited, is one of the most important aspects to be evaluated. The use of an inappropriate plating solvent could result in cracking, flaking and/or peeling off of the deposited material, which could cause burst releases of holmium during the intended use as a source for the sputtering processes.

Vascon et al. have already investigated the effects of the plating solvent on the molecular plating of neodymium [27,28]. The reported results indicated that solvents with higher boiling points or, equivalently, lower vapour pressures, should be preferred since they ensure smoother and crack-free films. The authors related the formation of surface cracking to the post-depositional drying process. In this stage, the obtained deposited layer is still permeated with the plating solvent, which tends to evaporate with a kinetics that depends on its vapour pressure. The faster the evaporation of the solvent, the more stress is induced into the deposited layer, promoting the development of cracks.

Casting-based methods, wherein the initial material, in a liquid state, is dispersed onto a substrate and allowed to dry, present a viable alternative to molecular plating. These techniques are generally rapid and quantitative; however, they yield non-uniform and heterogeneous layers, occasionally exhibiting inadequate adherence between the deposited material and the substrate. Consequently, they were considered unsuitable for the objectives of this study.

Methods grounded in the physical vapour deposition (PVD) process, including ion beam sputtering, thermal evaporation, pulsed laser deposition, and DC/RF magnetron sputtering, offer the ability to regulate the thickness of the deposited layer across a broader range, from μg cm^{-2} to mg cm^{-2}. This results in crack-free surfaces with superior homogeneity compared to molecular plating. Another notable advantage of these techniques is the enhanced control over the chemical speciation of the deposited species. However, two primary impediments render PVD methods unsuitable for inclusion in this study. Firstly, their yield is typically in the range of 10–20%, with slightly higher yields achievable through sputtering. This low efficiency is impractical when working with rare and costly materials, such as Ho-163, which is available in extremely limited quantities. Secondly, the PVD process involves the condensation of the vaporized starting material, particularly noteworthy in the case of radioactive Ho-163, onto all surfaces within the reactor chamber, beyond the substrate. Decontaminating these surfaces would be prohibitively expensive, if feasible at all. Furthermore, the radioprotection concerns are compounded by the necessity of maintaining high vacuum conditions within the reactor chamber. This mandates the use of non-conventional filtering systems, necessitating specific design, manufacture, and approval by local radioprotection authorities. The labor-intensive and costly nature of these procedures discouraged the adoption of PVD methods for the objectives of this research.

The aim of this work was to optimize and implement the molecular plating of natural holmium on a gold-plated copper substrate (corresponding to the cathode of the MP setup), by studying the effects of different plating solvents, with different vapour pressures, on the morphology of the plated films. Different techniques were applied to monitor the homogeneity and morphology of the produced films, such as Scanning Electron Microscopy (SEM), Energy Dispersive X-Ray Spectroscopy (EDX) and Radiographic Imaging (RI). Based on the obtained results, a holmium source was finally produced, which is going to be used for first HOLMES test experiments at the Genova INFN laboratory.

2. Experiments

2.1. Molecular plating (MP)

In this method, a salt of the element of interest, here $Ho(NO_3)_3 \cdot 5 H_2O$, is solubilized in a minimum amount of diluted acidic solution. This solution is then dissolved in an organic solvent, here referred to as plating solvent, forming a homogeneous electrolyte, referred to as plating solution. When a high voltage, several tens to some hundreds of volts, is applied to the plating solution, a current of a few mA is generated by the reduction of water (among other secondary reactions), according to the reaction (1):

$$2H_2O + 2e^- \rightarrow H_2 + 2OH^- \quad (1)$$

The production of hydroxide anions causes an increase in the pH near the cathode surface [29], until the conditions are favourable for the formation of holmium(III) hydroxide (2):

$$Ho^{3+} + 3OH^- \rightarrow Ho(OH)_3 \quad (2)$$

The combination of reaction (1) and (2) gives the complete deposition reaction:

$$2Ho^{3+} + 6H_2O + 6e^- \rightarrow 2Ho(OH)_3\downarrow + 3H_2 \quad (3)$$

Holmium(III) hydroxide has a low solubility in the organic solvents used for MP, and, when the solubility equilibrium is reached, it starts to precipitate onto the cathode. The quantity of hydrogen formed is small and does not interfere with the deposition process. Organic compounds of holmium, such as holmium carboxylates, $Ho(RCOO)_n$, can be formed by the reaction of Ho^{3+} with other species, resulting from the solvent's electrolytical decomposition [30], and co-precipitate on the cathode. Overall, the cathode is "plated" with molecular species of the element of interest, hence the name "molecular plating".

2.1.1. Molecular plating setups

Two setups were used in this work, one for the experiments performed to study the effects of plating solvents (hereafter solv. exps) and one to produce a holmium source for HOLMES test experiments (hereafter HOLMES exps). Fig. 1(a) shows the circuit diagram of both setups. A cell (hereafter MP cell) hosts two electrodes which are connected to a DC-power supply (Sorensen® programmable DC power supply XHR 600–1.7) allowing to regulate the output voltage from 0 V to 600 V. An amperometer and a voltmeter are connected, in series and in parallel, respectively, to the MP cell, to precisely monitor both current and voltage. All the depositions reported in this manuscript were performed in galvanostatic mode, i.e. a constant current was applied by varying the input voltage over the course of the MP experiments. The MP cell of the solv. exps, illustrated in Fig. 1 (b), consisted of two parts made of polyvinylidene fluoride (PVDF): a cylinder, schematically described in Fig. 1 (c), with an inner diameter of 25 mm ending with an aperture of 20 mm, and a base containing a 27 mm diameter circular copper cathode. The backing material, serving as substrate for the deposition, was placed on the top of the copper cathode. The sealing between the two parts, cylinder and base, was guaranteed by a fluorocarbon-based elastomer, Viton® FKM, O-ring. The anode, a 1 mm thick palladium wire coiled into a spiral with an outer diameter of 20 mm, was inserted from the top part of the cylinder and placed at about 20 mm above the cathode. In some experiments, when using more volatile solvents, a lid, also made of PVDF, was placed above the cylinder to minimize the evaporation of these solvents during deposition. The surface of the copper cathode was cleaned before each experiment with diluted HNO_3 and rinsed with ethanol.

The MP setup for the HOLMES exps had to be adapted to host the backing, schematically described in Fig. 2, consisting of a 65 mm diameter and 10 mm thick gold-coated copper disk, with a 2.5 mm rim, needed for fixing the holmium source in the ion implanter, and a 9 mm diameter circular hole in the middle. The surface of the disk adjacent to the inner hole has an angle of 45°. The total area available for the MP is about 29 cm^2.

Two samples were produced with this second setup. The first sample, HOLMES_1, was produced using an unpolished copper backing, coated with 50 nm of gold. This resulted in a rough surface with evident machining marks visible to the naked eye. For this reason, a second sample, HOLMES_2, was obtained using a copper backing that was polished after its manufacture. The copper backing was then coated with a 100 nm gold layer.

2.1.2. Molecular plating procedure

The starting holmium solutions of the reported experiments were prepared by solubilizing $Ho(NO_3)_3 \cdot 5\ H_2O$ (99.9%, Fisher Scientific, AG) in 0.01 M HNO_3 (69%, Sigma-Aldrich). The concentration of the starting holmium solution, hereafter Ho_{sol}, was calculated considering: 1) the total amount of holmium atoms to be implanted into the detector system of the HOLMES experiment, i.e. about 6.24×10^{16}, 2) a hypothetical yield of implantation of 0.8% and 3) that the total area of the backing used for the HOLMES exps is about 29 cm^2, while the area of the backings used for the solv. exps is 3.14 cm^2 (see later). Otherwise, the starting solution was spiked with trace amounts, few hundreds Bq, of ^{166m}Ho to monitor the yield of the deposition process and later perform radiographic imaging.

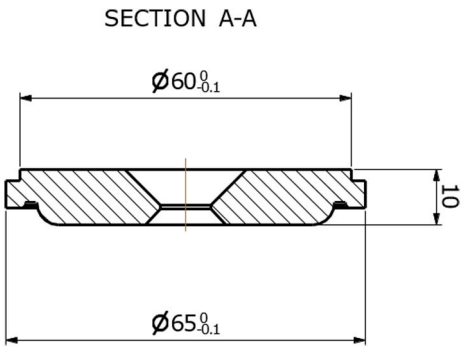

Fig. 2. Side section of the gold-coated copper backing used for the holmium deposition. (For interpretation of the references to colour in this figure legend, the reader is referred to the Web version of this article.)

2.1.2.1. Solv. exps. The concentration of Ho_{sol} of the solv. exps was 0.128 mg/μL. Thus, each solv. exp was performed dissolving 5 μL of the Ho_{sol} in 10 mL of the designated plating solvent. Different plating solvents, listed in Table 1, were selected based on their vapour pressure at room temperature, ranging from 0.17 kPa (N,N-Dimethylacetamide) to 30.80 kPa (Acetone) [31]. The obtained plating solution was then placed in the MP cell, where a current density of 0.8 mA × cm^{-2}, which is a value similar to the one used by Vascon, 0.7 mA × cm^{-2}, for the MP of samarium [18] and neodymium [28], was applied for 90 min. After, the plating solution was gently removed and the backing plated with

Table 1
List of plating solvents and their relative vapour pressure at room temperature.

Plating solvent	Vapour pressure at 25 °C [kPa] [31]
Acetone (100v%, BDH Prolabo)	30.80
Methanol (99.9v%, Fischer Chemical)	16.94
Ethanol (99.8v%, Fischer Chemical)	7.87
Isopropanol (100v%, AnalaR NORMAPUR®)	5.78
Isobutanol (99v%, Alfa Aesar®)	1.53
N,N-Dimethylformamide (DMF) (99.8v% Alfa Aesar®)	0.44
N,N-Dimethylacetamide (DMAc) (99 v% Alfa Aesar®)	0.17

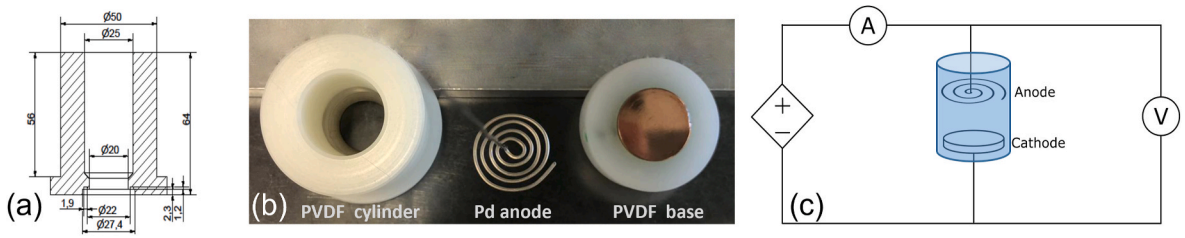

Fig. 1. (a) Photo illustrating the used MP cell made out of PVDF. (b) Schematic drawing of PVDF cylinder of the used MP cell. (c) Circuit diagram of the deposition setup used for the MP Backings for the solv. exps were produced by punching 20 mm diameter disks from a gold-coated copper foil, obtained by vapour phase deposition, using a Leybold Univex 450 vacuum evaporator, equipped with a quartz crystal microbalance allowing for precise measurements of the deposited layer thickness as well as of the coating rate. In particular, a 38 μm thick foil of copper (99.99%, Surepure Chemetals) was used as substrate. The copper foil was treated with diluted HNO_3 prior to each vaporization to remove the oxide layer present. The foil was polished successively with 10–20 μm, 4–8 μm and lastly 0–2 μm diamond pastes. After each polishing step, the foil was cleaned with ethanol and acetone. (For interpretation of the references to colour in this figure legend, the reader is referred to the Web version of this article.)

holmium, i.e. the holmium source, was removed, washed at room temperature with the same organic solvent as used for the plating. Subsequently the morphology and uniformity of the molecular-plated layer was investigated.

All the experiments were repeated at least twice to verify the reproducibility of the obtained results. In one repetition, it was noticed that, when performing SEM investigation soon after the MP, the deposited layer presented a greater number of interconnected cracks, resulting in an island-like structure, which was not detected in similar samples analysed several days after their production. This phenomenon was carefully investigated with an additional series of dedicated experiments, not reported here. It was concluded that the main cause of the island-like structure formation was a fast vaporization of the solvent still trapped in the deposited layer after MP. This event occurs even at ambient pressure when using solvents with relatively high vapour pressure, such as acetone and isobutanol. On the other hand, when using solvents with relatively low vapour pressure like DMF, it happens only when the sample is still impregnated with solvent and it undergoes a fast pressure drop, e.g. when introduced into the SEM chamber, where the pressure quickly drops down to 1×10^{-5}– 1×10^{-6} mbar. As previously mentioned in the introduction, similar phenomena were observed by Vascon et al. [27,28]. Based on this observation, all the solv. exps samples after MP were first left to dry in open air for 24 h. Then, they were gradually exposed to a low pressure, 1×10^{-1} mbar, in a desiccator filled with silica gel for another 24 h. This treatment was proven to successfully reduce the amount of solvent absorbed in the plated sample and minimize the stress on the deposited film when exposed to the low pressure of the SEM chamber.

2.1.2.2. HOLMES exps. The HOLMES exps, HOLMES_1 and HOLMES_2, were carried out using DMF as the plating solvent. In particular, the plating solution was obtained mixing 10 μL of $Ho(NO_3)_3 \cdot 5H_2O$ in 0.01 M HNO_3 (0.601 mg/μL) and 75 mL DMF (99v%, Emplura®). Additionally, the plating solution of HOLMES_1 was spiked with 1.64 kBq of ^{166m}Ho diluted in 5 μL of 0.01 M HNO_3, used as tracer. Both experiments were performed in galvanostatic mode keeping the current density between 1.4 mA/cm^2 and 1.9 mA/cm^2. A longer plating time, with respect to the solv. exps, of 180 min was selected to ensure high deposition yields. After the MP, both samples were immersed into fresh DMF for 5 min to remove any residue and debris that might have formed or settled on their surface during the MP. Subsequently, both samples were dried in air for several days and then gradually exposed to a weak vacuum in a glass desiccator filled with silica gel for five days.

2.2. Analysis and characterization methods

The yields of the MP experiments were evaluated by adding trace amounts of the γ-emitting radionuclide ^{166m}Ho to the plating solution and by measuring the γ count rate in the solution before and after the plating, by means of a coaxial high purity germanium detector (Falcon5000®, Canberra, crystal dimensions: 35 mm diameter and 52 mm length). Data were acquired using the Canberra acquisition interface module and the Genie2000® software package. The count rate was measured considering the most intensive γ-ray of ^{166m}Ho at 184.4 keV [32]. When using the same detector and the same measurement geometry, the yield could be calculated as:

$$yield = \frac{cps_{before} - cps_{after}}{cps_{before}}$$

where cps_{before} and cps_{after} stand for *count per seconds before* and *after* MP, respectively.

Similarly, the solutions used to wash the samples after MP were measured with the γ detector to estimate the material eventually detached from the surface of the obtained sample. This gave rough information about the adherence of the layer plated onto the backing.

Morphology investigations were carried out with scanning electron microscopy (SEM) using a Zeiss NVision-40 microscope. Elemental analysis of the deposited layer was studied by energy dispersive X-ray spectroscopy (EDX), using an Oxford Instruments X-Max^N 50 detector. The energy of the electron beam was set at 6 kV, allowing to minimize the emission of the gold L_α X-rays from the backing.

The spatial distribution of the deposited holmium on the source was investigated with radiographic imaging. A reusable Fujifilm imaging plate BAS-SR was exposed to the obtained samples, and then scanned with a GE Typhoon™ FLA 7000 Imaging Plate Reader, with a 25 μm pixel size. The image was saved as a 16-bit grey-value TIFF file. An exposure time of 48 h was chosen, matching the used ^{166m}Ho activity, in order to record data over the widest possible range of grey-values, without reaching any saturation.

3. Results

3.1. Solv. exps

Table 2 lists name codes of the experiments together with the applied plating solvents and the primary results expressed in terms of deposition yield and material loss during the washing of the obtained samples.

All the EDX investigations of the experiments listed in Table 2 gave similar results in terms of elemental composition of the deposited layer, i.e. oxygen and holmium were the main constituents with minor contents of carbon, indicating that the holmium could be precipitated as oxide, hydroxide and/or, carboxylate, see Fig. 3 for a representative example. Both gold and copper signals come from the used backing material, while the small nitrogen signal may be due to adsorption of species coming either from HNO_3, which was the solvent used to solubilise the holmium salt, or from the anionic component of the original holmium salt, i.e. $Ho(NO_3)_3 \cdot 5\ H_2O$.

EXP Ace: This experiment was performed using acetone as the plating solvent. The voltage was regulated between 400 V and 450 V, to keep the current density at the fixed value of 0.8 mA × cm^{-2}. A relatively low yield of 79.0% was measured for this experiment, with no significant loss of material during the washing stage. The radiographic image, Fig. 4 (a), reveals an inhomogeneous deposition with regions characterized by very high concentration of holmium (dark area). The SEM analysis of this sample confirms the inhomogeneity of the deposition, showing in addition that a large part of the backing is not covered by holmium species, Fig. 4 (b). Moreover, the deposited layer shows formation of agglomerates with poor adherence, Fig. 4 (c).

EXP MeOH: This experiment, realized using methanol as a plating solvent, showed a different current/voltage trend, compared to all other reported experiments. In fact, the average voltage needed to keep the current density at 0.8 mA × cm^{-2} was 12 V, much smaller than the 50 V–2000 V generally required for MP [7]. Despite this unusual behaviour, the yield reached 99.2% and the losses following the washing remained low, about 1.8%. The radiographic investigation, Fig. 5 (a), shows a distribution more concentrated in the perimeter rather than the central area. The SEM analysis, Fig. 5(b–d), shows a different kind of deposit compared to EXP Ace, made of spherical beads packed up into aggregates arranged in a dendritic macrostructure.

Table 2
Codes, plating solvents and results in terms of deposition yield and material loss during the washing stage of the MP experiments.

Code	Plating solvent	Yield/%	Loss/%
EXP Ace	Acetone	79.0	0
EXP MeOH	Methanol	99.2	1.8
EXP EtOH	Ethanol	82.6	0
EXP i-PrOH	Isopropanol	99.9	14.8
EXP i-BuOH	Isobutanol	98.1	0
EXP DMF	DMF	99.4	1.8
EXP DMAc	DMAc	96.5	0

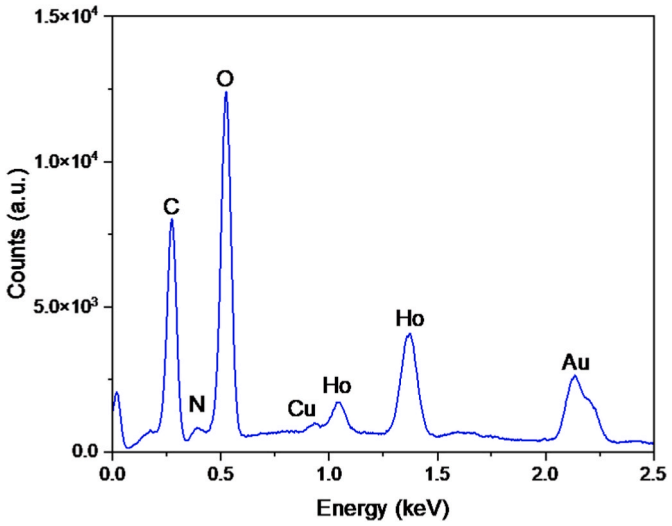

Fig. 3. Representative example of an EDX-spectrum obtained in the investigations, from EXP Ace.

EXP EtOH: The yield reached in this experiment, obtained with an average applied voltage of 50 V, was 82.6% with 0% loss following the sample washing. From the radiographic image, Fig. 6 (a), a significantly more pronounced deposition in the outer rim region can be seen.

The SEM analysis, Fig. 6(b–d), reveals a deposited layer made of interconnected "lumps", and spheres similar to the microstructure of EXP MeOH, forming an island-like macrostructure. Neither flaking nor peeling off was visible.

EXP i-PrOH: Although this experiment, performed using isopropanol and applying a potential between 130 V and 170 V, recorded an almost quantitative deposition of 99.9%, the adherence of the deposited layer was poor, resulting in 14.8% of material loss after the washing step. The deposition was very inhomogeneous, as shown by the radiographic image in Fig. 7 (a), with spots of more concentrated activity randomly distributed on the sample surface.

The SEM image, Fig. 7 (b), obtained with 150x magnification, revealed an "island-like" structure, with large, interconnected cracks. Those "islands" are inclined to flake and peel off, indicating a very poor adherence of the deposited film. This could explain the loss of material during the sample washing, leaving large parts of the backing surface completely uncovered.

EXP i-BuOH: The voltage applied was between 260 V and 300 V. The yield measured, when using isobutanol as plating solvent, was 98.1% while the loss associated with the sample washing was close to 0%. The radiography, Fig. 8 (a), reveals an overall fairly good homogeneity of the deposition, with the exception of some spots concentrating a large part of the overall activity. These spots are also observed as bright spots on the photographic image of the sample, Fig. 8 (b).

The microstructure revealed by the SEM investigation, Fig. 8 (c,d), is more homogeneous, uniform and smoother compared to EXP EtOH and EXP MeOH, without formations of lumps. Although there is a high density of interconnected cracks forming different sizes of island-like structures, no significant peeling off can be noted, and the backing results to be completely covered by the deposited layer.

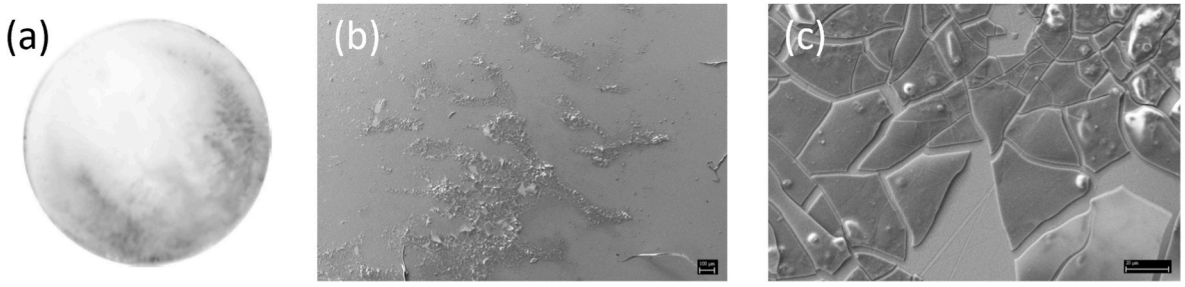

Fig. 4. (a) Radiographic image, after 48 h of exposure, of sample EXP Ace. SEM images of the sample EXP Ace at (b) 40x (bar scale 100 μm)and (c) 600x (bar scale 10 μm)magnification.

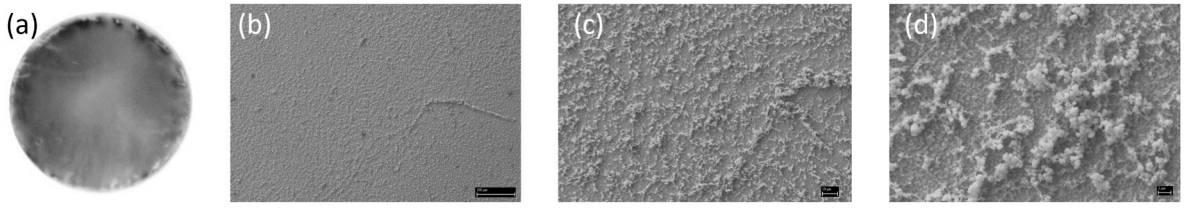

Fig. 5. (a) Radiographic image, after 48 h of exposure, of sample EXP MeOH. SEM images of the sample EXP MeOH at (b) 150x (bar scale 100 μm), (c) 600x (bar scale 10 μm)and (d) 2500x (bar scale 2 μm)magnification.

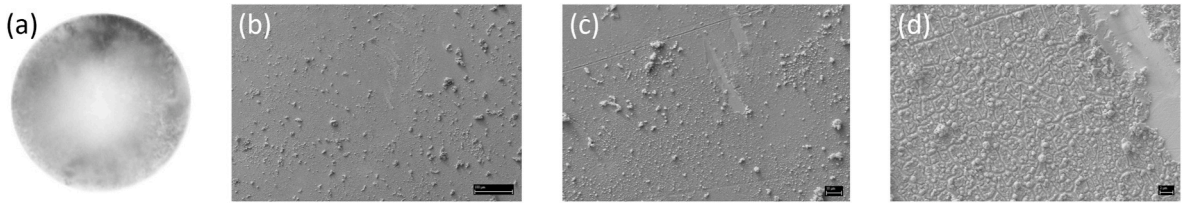

Fig. 6. (a)Radiographic image of sample EXP EtOH. SEM images of the sample EXP EtOH at (b) 150x (bar scale 100 μm), (c) 600x (bar scale 10 μm)and (d) 2500x (bar scale 2 μm)magnification.

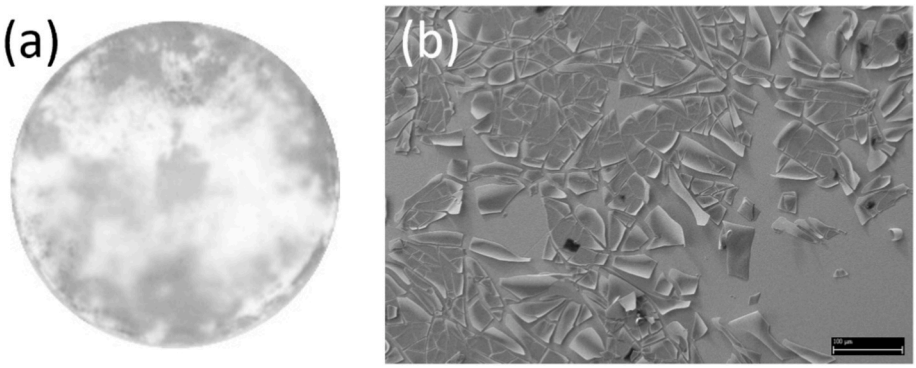

Fig. 7. (a)Radiographic image of sample EXP i-PrOH. (b) SEM image of the sample EXP i-PrOH at 150x magnification (bar scale 100 μm).

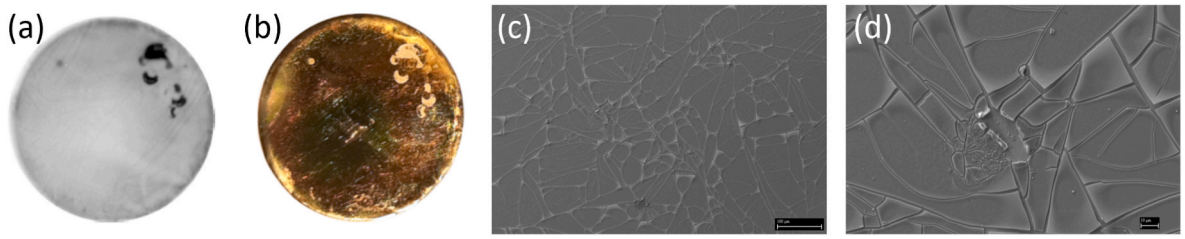

Fig. 8. (a) Radiographic and (b) photographic image of sample i-BuOH. SEM images of the sample EXP i-BuOH at (c) 150x (bar scale 100 μm) and (d) 600x magnification (bar scale 10 μm).

EXP DMF: An average voltage of 100 V was applied in this experiment. The yield and material loss of this experiment were 99.4% and 1.8%, respectively. The sample was characterized by a very uniform deposition, Fig. 9 (a), with only few slightly concentrated spots in the peripheral region. The SEM investigation, Fig. 9(b–d), revealed supporting information, namely, low amounts of small and isolated cracks without either flaking or peeling off of the deposited material.

EXP DMAc: This experiment, obtained using DMAc with a similar applied voltage of the **EXP DMF**, gave a yield of 96.5% and the loss resulting from the washing was close to 0%. The overall deposition, evaluated by radiography as shown in Fig. 10 (a), was homogeneous, with a slightly more concentrated region in the centre of the sample.

No extended cracks are visible in the SEM image at 150x magnification, Fig. 10 (b). Nonetheless, some flaking of the deposited layer is visible in the SEM image with 600x magnification, Fig. 10 (c). Furthermore, some clusters with different sizes, ranging from some hundreds of nm to 10 μm, are randomly formed on the top of the deposited layer.

3.2. HOLMES exps

HOLMES_1: An average voltage of 80 V was applied for 180 min. The deposition yield measured for this experiment was 99.97%. The radiographic image (obtained with 43 h exposure), Fig. 11 (a), shows a very homogeneous deposition. A slightly darker area can be seen at the borders of the source. However, this is not entirely connected with a higher concentration of deposited holmium but with the geometry of both the backing and the MP cell. In fact, the inner darker area resembles the inner edge of the backing, where the surface starts to slant inwards, see Fig. 2. On the other hand, the darker area in the periphery of the sample is probably originated by a slightly higher concentration of holmium in correspondence of the contact area between the backing and the Viton® FKM O-ring used for sealing of the MP cell.

The SEM images, Fig. 11(b–d), reveal a small number of cracks which are not interconnected. It is also possible to notice that the deposition follows the machining marks of the backing surface. This last observation revealed the need for polishing the copper surface before coating it with gold, to avoid the formation of oriented and/or preferential deposition areas.

In Fig. 12, the EDX investigation of sample HOLMES_1 shows, besides the signals of copper and gold coming from the backing material, a deposition rich in holmium and oxygen with some carbon and very small amounts of nitrogen and fluorine. The latter could result from the partial dissolution of the Viton® FKM O-ring used to seal the two parts of the MP cell.

HOLMES_2: Also in this case, the applied average voltage was 80 V. The copper surface of the backing used for this sample was polished before being coated with gold. This resulted in a much smoother surface, as it is possible to appreciate in the SEM picture (81x magnification) reported in Fig. 13 (a).

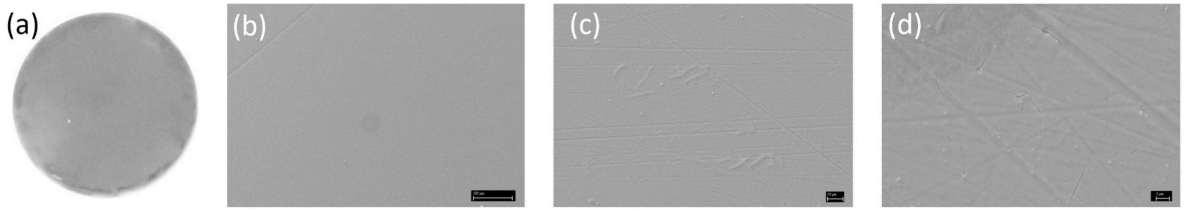

Fig. 9. (a) Radiographic image of sample EXP DMF. SEM images of the sample EXP DMF at (b) 150x (bar scale 100 μm), (c) 600x (bar scale 10 μm) and (d) 2500x (bar scale 2 μm) magnification.

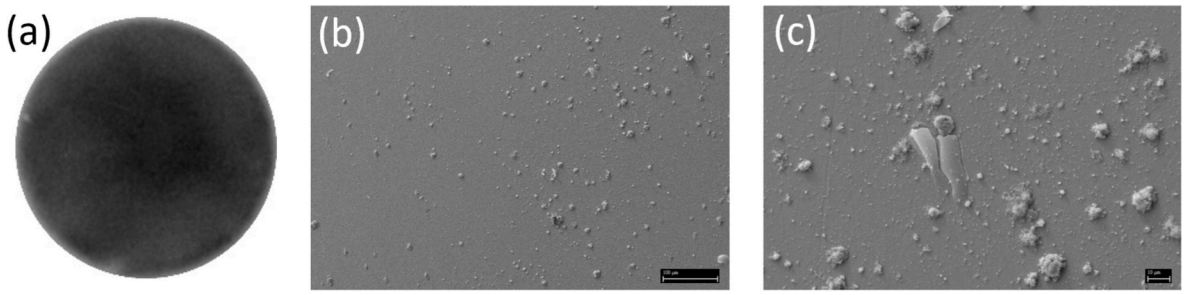

Fig. 10. (a) Radiographic image of sample EXP DMAc. SEM images of the sample EXP DMAc at (b) 150x (bar scale 100 μm) and (c) 600x (bar scale 10 μm) magnification.

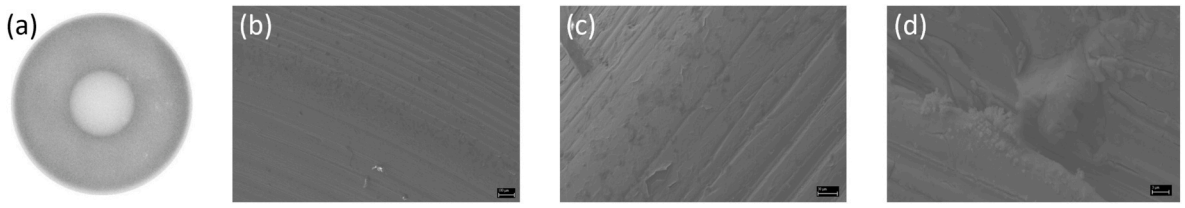

Fig. 11. (a) Radiographic image of sample HOLMES_1. SEM pictures of sample HOLMES_1 at (b) 64x (bar scale 100 μm), (c) 256x (bar scale 30 μm) and (d) 2200x (bar scale 3 μm) magnification.

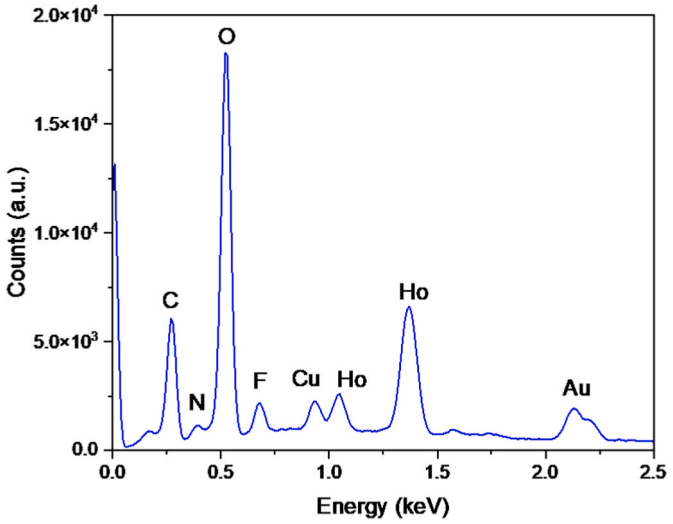

Fig. 12. EDX spectrum of a selected point of interest in the deposit of sample HOLMES_1 exp.

The SEM images at 1270x and 4230x magnification, Fig. 13 (b,c), show that the deposited area is very homogeneous with no significant cracks nor island structures, and most importantly, with no peeling off of the deposited layer (the bright scratches are due to mechanical handling of the sample).

The EDX analysis of this sample, not shown here, gave similar results to sample HOLMES_1, i.e. an elemental composition rich in both holmium and oxygen, with some trace of carbon, nitrogen and fluorine.

4. Discussion

A first important output of the plating exp series was the establishment of a procedure for reducing the concentration of solvent absorbed by the deposited layer after MP. This minimized the stress on the deposited layer when subjected to a fast decrease of pressure, preventing misinterpretations of the SEM results. These inputs were used to implement a protocol for performing the MP at constant current density, aiming to study the influence of plating solvents with different vapour pressure, on both yield of deposition and morphology of the resulting plated layer.

The first experiment presented in this manuscript, EXP Ace, performed using acetone as the plating solvent, the most volatile solvent used in this work, showed the lowest yield among the reported experiments. It is clear that the deposition was insufficient and characterized by several interconnected cracks resulting in an “island-like” microstructure. This could be due to the high vaporization rate of the solvent causing the fragmentation and eventually the detachment of the deposited layer.

The use of methanol as plating solvent, EXP MeOH, also led to an atypical result obtained at a much lower voltage than usually achieved in molecular plating. Despite that, the experiment resulted in a high yield with low material loss during the cleaning step, indicating a good adherence of the deposited layer, which completely covered the

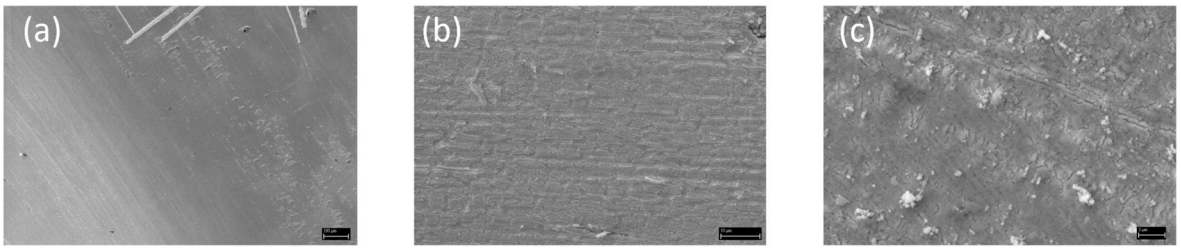

Fig. 13. SEM pictures of sample HOLMES_2 at (a) 81x (bar scale 100 μm), (b) 1270x (bar scale 10 μm) and (c) 4230x (bar scale 2 μm) magnification.

backing, although not uniformly.

The MP using ethanol, EXP EtOH, resulted in a deposited layer with a microstructure similar to EXP MeOH, although with lower adherence to the backing. The transition to solvents with lower vapour pressure, such as isopropanol and isobutanol, resulted in molecular plating with higher yields but with inhomogeneous layers with bad adherence. Much better results, in terms of deposition yields, morphology and adherence of the deposited layers, were obtained when using DMF and DMAc, the least volatile solvents used in this work. In both cases, a nearly quantitative deposition yield was achieved, and the resulting layer presented a smooth surface without interconnected cracks developing into flaking and peeling off, which could result in material loss during the envisaged HOLMES experiments. Very likely, the relatively low vapour pressure allowed a smoother and gradual vaporization of both DMF and DMAc, minimizing mechanical stress in the resulting deposited film. However, some local cracks were formed. This indicates the need of optimizing the drying process even further, for instance, by increasing the vacuum strength in more steps and for longer times. In addition, the resulting plated sample could be gently heated up to ensure a more complete vaporization of the solvent. One additional source of inhomogeneity may arise from variations in the electric field intensity between the electrodes, attributable to the utilization of a stationary coiled spiral as the anode. As documented, for instance, in Ref. [33], achieving a more uniform electric field—resulting in molecular plated layers of greater uniformity—can be realized by employing either more densely packed and continuous surfaces, such as a disk, or by introducing rotation to the anode during the plating process.

Regrettably, both of these solutions proved impractical within our laboratory setting, primarily due to the requirement for an excessively large anode, approximately 60 mm in diameter, mandated by the HOLMES experiments. Attempts using a 60 mm diameter gold disk as the anode were unsuccessful, primarily due to structural failure at the weld joint connecting the disk and the wire used for electrical connection. Conversely, the attainment of a completely flat anode was unfeasible, precluding the use of a rotor.

Based on the results reported above, we decided to produce the sample for the HOLMES experiments using DMF as a plating solvent. In particular, we produced two samples, HOLMES_1 and HOLMES_2. These samples had an almost ten times larger surface than the ones produced in the solv. exp series (about 29 cm^2 for the HOLMES exps compared to 3.14 cm^2 for the solv. exps). HOLMES_1 achieved an almost quantitative deposition, indicating that the developed deposition procedure is also suitable for the production of large samples. The deposited layer, which showed a very good adherence, was characterized by some micrometric non-interconnected cracks, and a complete absence of peeling off. However, the non-smooth surface of the used copper backing led to an inhomogeneously deposited layer, characterized by visible grooves. In HOLMES_2 the use of a polished copper backing resulted in an equivalently good deposition (in terms of both, deposition yield and adherence of the deposited layer), but also with a much better homogeneity. Based on these results, the HOLMES_2 sample was selected to be used in the forthcoming preparatory HOLMES experiments for the sputtering.

5. Conclusions

A procedure for the molecular plating of holmium onto a gold-coated copper cathode was developed, investigating the effects of plating solvents with different vapour pressures on both, deposition yield and morphology of the deposited layers. The best result was obtained using DMF as plating solvent and applying a specific procedure to dry the obtained samples after molecular plating. The developed method allowed to obtain almost quantitative deposition yields, homogeneously deposited holmium layers with a stable microstructure and very good adherence to the gold-coated copper cathode, despite the use of a non-ideal anode, i.e., a stationary platinum wire coiled into a spiral. Following the developed method, a first holmium source was produced for testing the ion implanter developed at the Genova INFN laboratory.

CRediT authorship contribution statement

N. Cerboni: Validation, Investigation, Writing – review & editing. **G. de Bodin-de Galembert:** Development or design of, Methodology, creation of models, Validation, Investigation, Data curation, Writing – review & editing. **M. De Gerone:** Conceptualization, Writing – review & editing. **G. Gallucci:** Conceptualization, Writing – review & editing. **E. Müller:** Validation, Investigation, Writing – review & editing. **A. Nucciotti:** Conceptualization, Writing – review & editing. **P. Steinegger:** Resources, Supervision, Management and coordination responsibility for the research activity planning and execution. **E.A. Maugeri:** Conceptualization, Development or design of, Methodology, creation of models, Validation, Investigation, Data curation, Writing – original draft, Supervision, Management and coordination responsibility for the research activity planning and execution.

Declaration of competing interest

The authors declare that they have no known competing financial interests or personal relationships that could have appeared to influence the work reported in this paper.

Data availability

Data will be made available on request.

Acknowledgements

The authors would like to thank Dr. P. Trtik for the assistance with the radiographic imaging investigation.

References

[1] B. Alpert, M. Balata, D. Bennett, M. Biasotti, C. Boragno, C. Brofferio, V. Ceriale, D. Corsini, P.K. Day, M. De Gerone, R. Dressler, M. Faverzani, E. Ferri, J. Fowler, F. Gatti, A. Giachero, J. Hays-Wehle, S. Heinitz, G. Hilton, U. Koster, M. Lusignoli, M. Maino, J. Mates, S. Nisi, R. Nizzolo, A. Nucciotti, G. Pessina, G. Pizzigoni, A. Puiu, S. Ragazzi, C. Reintsema, M.R. Gomes, D. Schmidt, D. Schumann, M. Sisti, D. Swetz, F. Terranova, J. Ullom, HOLMES the electron capture decay of ^{163}Ho to measure the electron neutrino mass with sub-eV sensitivity, Europ. Phys. J. C 75 (3) (2015) 112.

[2] A. De Rújula, M. Lusignoli, Calorimetric measurements of ^{163}holmium decay as tools to determine the electron neutrino mass, Phys. Lett. B 118 (4) (1982) 429–434.

[3] S. Heinitz, N. Kivel, D. Schumann, U. Köster, M. Balata, M. Biasotti, V. Ceriale, M. De Gerone, M. Faverzani, E. Ferri, G. Gallucci, F. Gatti, A. Giachero, S. Nisi, A. Nucciotti, A. Orlando, G. Pessina, A. Puiu, S. Ragazzi, Production and separation of ^{163}Ho for nuclear physics experiments, PLoS One 13 (8) (2018), e0200910.

[4] M. De Gerone, A. Bevilacqua, M. Borghesi, N. Cerboni, G. Ceruti, G. De Bodin De Galembert, M. Faverzani, M. Fedkevych, E. Ferri, G. Gallucci, F. Gatti, A. Giachero, E. Maugeri, P. Manfrinetti, A. Nucciotti, L. Parodi, G. Pessina, S. Ragazzi, D. Schumann, F. Siccardi, Development and commissioning of the ion implanter for the HOLMES experiment, Nucl. Instrum. Methods Phys. Res., Sect. A 1051 (2023), 168168.

[5] M. De Gerone, M. Biasotti, V. Ceriale, R. Dressler, M. Faverzani, E. Ferri, G. Gallucci, F. Gatti, A. Giachero, S. Heinitz, P. Manfrinetti, A. Nucciotti, A. Orlando, A. Provino, A. Puiu, D. Schumann, 163Ho distillation and implantation for the HOLMES experiment, Nucl. Instrum. Methods Phys. Res., Sect. A 936 (2019) 220–221.

[6] G. Gallucci, M. Biasotti, V. Ceriale, M. De Gerone, M. Faverzani, E. Ferri, F. Gatti, A. Giachero, P. Manfrinetti, A. Nucciotti, A. Orlando, A. Provino, A. Puiu, ^{163}Ho distillation and implantation for HOLMES experiment, J. Low Temp. Phys. 194 (5) (2019) 453–459.

[7] W. Parker, R. Falk, Molecular plating: a method for the electrolytic formation of thin inorganic films, Nucl. Instrum. Methods 16 (1962) 355–357.

[8] S. Sadi, A. Paulenova, P.R. Watson, W. Loveland, Growth and surface morphology of uranium films during molecular plating, Nucl. Instrum. Methods Phys. Res., Sect. A 655 (1) (2011) 80–84.

[9] J.P. Greene, R.V.F. Janssens, I. Ahmad, Preparation of actinide targets by molecular plating for Coulomb excitation studies at ATLAS, Nucl. Instrum. Methods Phys. Res. Sect. A Accel. Spectrom. Detect. Assoc. Equip. 438 (1) (1999) 119–123.

[10] Q. Zhi, G. Junsheng, G. Zaiguo, Preparation of the thicker americium targets by molecular plating, Appl. Radiat. Isot. 54 (5) (2001) 741–744.

[11] J.P. Greene, I. Ahmad, Molecular plating of actinides on thin backings, Nucl. Instrum. Methods Phys. Res. Sect. A Accel. Spectrom. Detect. Assoc. Equip. 590 (1–3) (2008) 131–133.
[12] R. Haas, M. Hufnagel, R. Abrosimov, C.E. Düllmann, D. Krupp, C. Mokry, D. Renisch, J. Runke, U.W. Scherer, Alpha spectrometric characterization of thin ^{233}U sources for $^{229(m)}$Th production, Radiochim, Acta 108 (12) (2020) 923–941.
[13] G. Sibbens, A. Moens, R. Eykens, D. Vanleeuw, F. Kehoe, H. Kühn, R. Wynants, J. Heyse, A. Plompen, R. Jakopič, S. Richter, Y. Aregbe, Preparation of ^{240}Pu and ^{242}Pu targets to improve cross-section measurements for advanced reactors and fuel cycles, J. Radioanal. Nucl. Chem. 299 (2) (2014) 1093–1098.
[14] W. Parker, H. Bildstein, N. Getoff, Molecular plating I, a rapid and quantitative method for the electrodeposition of thorium and uranium, Nucl. Instrum. Methods 26 (1964) 55–60.
[15] A. Vascon, Molecular plating of thin lanthanide layers with improved material properties for nuclear applications, Fachbereich Chemie, Pharmazie und Geowissenschaften, Johannes Gutenberg-Universität, Mainz, 2013.
[16] K.G. Myhre, J.C. Delashmitt, N.J. Sims, S.M.V. Cleve, R.A. Boll, Samarium thin films molecular plated from N,N-dimethylformamide characterized by XPS, Surf. Sci. Spectra 25 (2) (2018), 024003.
[17] E.A. Maugeri, S. Heinitz, R. Dressler, M. Barbagallo, N. Kivel, D. Schumann, M. Ayranov, A. Musumarra, M. Gai, N. Colonna, M. Paul, S. Halfon, L. Cosentino, P. Finocchiaro, A. Pappalardo, Preparation of ^{7}Be targets for nuclear astrophysics research, J. Inst. Met. 12 (2) (2017), P02016.
[18] A. Vascon, N. Wiehl, T. Reich, J. Drebert, K. Eberhardt, C.E. Düllmann, The performance of thin layers produced by molecular plating as α-particle sources, Nucl. Instrum. Methods Phys. Res., Sect. A 721 (2013) 35–44.
[19] Z. Talip, R. Dressler, B. Schacherl, J.-C. David, C. Vockenhuber, D. Schumann, Radiochemical determination of long-lived radionuclides in proton-irradiated heavy metal targets: Part II tungsten, Anal. Chem. 93 (31) (2021) 10798–10806.
[20] Z. Talip, S. Pfister, R. Dressler, J.C. David, A. Vögele, P. Vontobel, R. Michel, D. Schumann, Analysis of the ^{148}Gd and ^{154}Dy content in proton-irradiated lead targets, Anal. Chem. 89 (12) (2017) 6861–6869.
[21] Z. Talip, R. Dressler, J.C. David, C. Vockenhuber, E. Müller Gubler, A. Vögele, E. Strub, P. Vontobel, D. Schumann, Radiochemical determination of long-lived radionuclides in proton-irradiated heavy-metal targets: Part I—tantalum, Anal. Chem. 89 (24) (2017) 13541–13549.
[22] A. Vascon, J. Runke, N. Trautmann, B. Cremer, K. Eberhardt, C.E. Düllmann, Quantitative molecular plating of large-area ^{242}Pu targets with improved layer properties, Appl. Radiat. Isot. 95 (2015) 36–43.
[23] S. Heinitz, E.A. Maugeri, D. Schumann, R. Dressler, N. Kivel, C. Guerrero, U. Köster, M. Tessler, M. Paul, S. Halfon, Production, separation and target preparation of ^{171}Tm and ^{147}Pm for neutron cross section measurements, Radiochim. Acta (2017) 801.
[24] K. Eberhardt, M. Schädel, E. Schimpf, P. Thörle, N. Trautmann, Preparation of targets by electrodeposition for heavy element studies, in: Nuclear Instruments and Methods in Physics Research, Section A: Accelerators, Spectrometers, Detectors and Associated Equipment, 2004, pp. 208–213.
[25] I. Usoltsev, R. Eichler, R. Dressler, D. Piguet, D. Wittwer, A. Türler, R. Brütsch, E. A. Olsen, J.P. Omtvedt, A. Semchenkov, Preparation of Pd-based intermetallic targets for high intensity irradiations, Nucl. Instrum. Methods Phys. Res., Sect. A 691 (2012) 5–9.
[26] Y.V. Lobanov, G.V. Buklanov, F.S. Abdullin, A.N. Polyakov, I.V. Shirokovsky, Y. S. Tsyganov, V.K. Utyonkov, Targets of uranium, plutonium, and curium for heavy-element research, Nucl. Instrum. Methods Phys. Res. Sect. A Accel. Spectrom. Detect. Assoc. Equip. 397 (1) (1997) 26–29.
[27] A. Vascon, S. Santi, A.A. Isse, A. Kühnle, T. Reich, J. Drebert, K. Eberhardt, C. E. Düllmann, Smooth crack-free targets for nuclear applications produced by molecular plating, Nucl. Instrum. Methods Phys. Res., Sect. A 714 (2013) 163–175.
[28] A. Vascon, S. Santi, A.A. Isse, T. Reich, J. Drebert, H. Christ, K. Eberhardt, C. E. Düllmann, Fundamental aspects of molecular plating and production of smooth crack-free Nd targets, J. Radioanal. Nucl. Chem. 299 (2) (2014) 1085–1091.
[29] P.G. Hansen, The conditions for electrodeposition of insoluble hydroxides at a cathode surface: a theoretical investigation, J. Inorg. Nucl. Chem. 12 (1) (1959) 30–37.
[30] A. Vascon, S. Santi, A.A. Isse, T. Reich, J. Drebert, H. Christ, C.E. Duellmann, K. Eberhardt, Elucidation of constant current density molecular plating, Nucl. Instrum. Methods Phys. Res. A 696 (2012) 180–191.
[31] David R. Lide, H.V. Kehiaian, CRC Handbook of Thermophysical and Thermochemical Data, CRC Press, 1994.
[32] Y. Hino, S. Matui, T. Yamada, N. Takeuchi, K. Onoma, S. Iwamoto, H. Kogure, Absolute measurement of ^{166m}Ho radioactivity and development of sealed sources for standardization of γ-ray emitting nuclides, Appl. Radiat. Isot. 52 (3) (2000) 545–549.
[33] Y. He, L. Han, C. Wang, Q. Chen, M.M. Sartin, G. Li, R. Hu, J. Tu, X. Xie, Y. Yang, F.-Z. Yang, D. Zhan, Molecular plating of actinide compounds on wafer-scale aluminum substrate, J. Alloys Compd. 878 (2021), 160393.